65

New Process of Developing Nanocrytalline Fecr for Fuel Cell Application

Darwin Sebayang, Maizlinda Izwana, Asraf Othman, Dafit Feriyanto, Deni S. Khaerudini & Hendi Saryanto

ABSTRACT

FeCr alloy were developed as a replacement of ceramic interconnect, they are favored because their moderate oxidation resistance and fairly good corrosion resistance provided by the formation of Cr_2O_3 scale in the presence of oxidant. Therefore the FeCr alloy compatible for SOFC application. The aim of this project is to conduct the research on the effect of each process in the high temperature oxidation for SOFC application of FeCr alloy. The new process of this research is combining the ball milling process with holding time 15 h, 20 h, 40 h, 60 h, and 80 h, hot pressing at pressure of 25 MPa and temperature of 1000 ^{0}C with sample name HP1000, spark plasma sintering at pressure of 10 MPa and temperature of 800 ^{0}C and 900 ^{0}C with sample name SPS800 and SPS900 and surface treatment via ion implantation by La as implant to obtain material that having good electrical resistance, good microstucture and good in high temperature oxidation for SOFC application. In the ball milling process the smallest crystallite size in milling time 60 h, and the SEM micrograph not identifies the crack and voids in the surface of consolidated specimens. Surface treatment via La-implanted effective to obtain a better result at consolidation process, surface treatment process and electrical analysis than commercial materials. The contribution of La implantation is also essential for the effectiveness of internal to external oxidation transition.

Keywords: FeCr, SOFC, new process and ion implantation.

INTRODUCTION

Fuel Cell is generally regarded to be the central importance for the transformation the so-called hydrogen economy. One of the promising fuel cell systems in future is Solid Oxide Fuel Cell (SOFC) due to the high –density power generation device. Solid oxide posses sufficiently high ionic conductivity at the elevated temperature so that SOFC must operate at the temperature range of 800- 1000^{0}C. The material in nano range size have many advantages to becoming SOFC application such as enhanced diffusivity, improved ductility, reduced density and modulus, high electrical resistance, high thermal expansion coefficient, lower thermal conductivity, and superior soft magnetic properties if in comparison with conventional coarse-grained materials. Exploration of new energy resources seems to be challenging task for the future. One of the most promising and attention fuel cell systems seems to be solid oxide fuel cell (SOFC) because of its potential for becoming an efficient and high energy-density power generation device [1, 2].

Metallic materials as SOFC application have many advantages of a high electronic conductivity, lower cost and easier fabrication [2]. Metal alloy are not capable of performing adequately over extended periods. This is challenging because the interconnector is exposed to both oxidizing condition at the cathode and reducing condition at the anode. Metal alloy with specific physical and mechanical properties and retains their strength at the elevated temperature that could be applied successfully as a fuel cell interconnects.

Metal alloys have long been considered as potential candidates for high temperature application because their strength to weight ratio [3]. New FeCr based alloys have recently been developed specially for SOFC applications. These materials seems to be sufficiently good for most of the envisaged SOFC application, however, its still important to improving the result with designed the composition of FeCr alloys.

Mechanical alloying had been introduced with ball milling process, and SPS technique to produce the bulk FeCr alloy, since the process is capable of control to producing many metallic alloy with a perfectly controlled degree of densification. Microstructure with near theoretical density over 99% at relatively lower sintering temperature (200 to 500 ^{0}C) than the temperature using in conventional HP process [4]. SPS sintering can be completed in a short period of 5 to 20 minutes including temperature rise and holding times [4].

Ion implantation method used as surface treatment process, ion implantation for the modification of surface properties of materials by insertion of accelerated atoms within the firs atomic layer into solid substrate [3]. Ion implantation is widely used to modify the oxidation behavior to the surface of the alloys, Ion implantation will allow the introducing of a controlled reactive element (RE) concentration into the alloys surface to modification of the corrosion behavior of the metal surface. The minor addition of RE such as La, Y, Ti, Hf and Ce could significantly improve the spallation resistance of these oxide scale under oxidizing and reducing conditions and inhibits further by isothermal and thermal cycling oxidation [3, 5].

The main aim of this research to investigate the effects of each process in the high temperature oxidation for SOFC application. To more understanding, the available high Fe and Cr ferritic model alloys were prepared into the test program. Characterization by using X-ray diffraction (XRD), scanning electron microscopy (SEM), and energy dispersive X-ray spectroscopy (EDX) to investigate the microstructure, phase and the formation of the oxide layer.

METHODOLOGY

Preparation material on the research

The raw material is commercially available powders of iron (320 mesh and purity >99.9%) and chromium (320 mesh and purity >99.8%). The nominal weight composition of alloyed Fe and Cr closed to 80:20 wt%.

Preparation

Milling

Milling process has done with the firs stage is the mixtures were sealed in a 250 ml hardened stainless steel vial. The ratio was fixed 20:1 weight ratio of ball to powder. Mechanical alloying

process was conducted in different milling time for 7 h, 15 h, 20 h, 40 h, 60 h, and 80 h in RETCH PM400 planetary ball mill and the rotation speed of 300 rpm.

Hot pressing and SPS process

The consolidation process there are three parameter should be specified that temperature, compaction pressure and soaking time of the process. Hot pressing were poured into a cylinder shape and pressed at 25 MPa with a diameter of 33 mm and thickness of 4-5 mm by using vacuum hot press machine and the sintering process was conducted in temperature 1000 ^{0}C at heating and cooling rate of 20 ^{0}C/min with the holding time 45 minutes. Spark plasma sintering process was conducted with temperature of 800 ^{0}C and 900 ^{0}C. SPS process was conducted by using the SPS Model 10-3 apparatus at a loading pressure of 10 MPa and cooling rate of 400^{0}C/min with significant short holding time of 5 minutes.

Surface treatment process

Ion implantation of lanthanum dopants with nominal doses 1x10^{17} ions/cm^2 was undertaken using 10 KeV acceleration potential with beam current density of 10 μA/cm^2 and 20 kV extraction voltages.

Oxidation experimental

The oxidation test must be examined under conditions which resemble SOFC operational conditions. In this study Oxidation test carried out using a resistance box furnace in air atmospheric pressure to cover the extreme conditions. In this work the cyclic oxidation test was conducted at 900 ^{0}C and 1100 ^{0}C. The experiment was designed at 5 cycles which each cycle consist of 20 h of soaking period. The sample weight change which measured by an electronic microbalance with resolution of 0.01 mg were recorded after each cycle in order to plot the weight gain and oxidation graph.

ANALYSIS

Determine of crystallite size and strain of materials.

Determining the crystallite size and strain of milled and unmilled powders was conducted by the Williamson-Hall Method [6]:

$$\varepsilon_{strain} = \frac{B}{4\tan\theta} \tag{1}$$

$$B\cos\theta = \frac{K\lambda}{D} + 4\varepsilon\sin\theta \tag{2}$$

Where: D = Volume weighted crystallite size
K = scherrer constant (0.87-1.0)

λ = the wave length of the radiation
B = FWHM of refletion peaks located at 2
ε_{strain} = weight average strain

SEM analysis.

SEM carried out in laboratory of materials with brands machine is SEM JEOL JSM-6380LA which equipped with EDS. SEM is very high image resolution of the sample surface, the resolution in about 1-5 nm.

XRD analysis

The XRD analyses were determine using a Bruker model D8 advance XRD. From Brags angle (2) in the range of 30° to 90° at a scene rate of 0.02°/min to provide adequate sampling of the peaks height (FWHM).

Electrical resistivity analysis.

Electrical resistivity was evaluated by using the standard two point electrical measurement to obtain electrical current-voltage curve of the oxidized samples. The resistivity was conducted under the static air condition after exposing thermal cycles for 100 h of different oxidation temperatures. The measurement were carried out at the Microelectronics and Nanotechnology - Shamsudin research centre (MiNT-SRC) of UTHM. The various samples are designated as shown in following Table 1.

Table 1: The investigated alloy designation

Alloy designation	Sample name	Major features
$Fe_{80}Cr_{20}$ 15 h	$Fe_{80}Cr_{20}$ 15 h	Milled 15 h and hot compacted
$Fe_{80}Cr_{20}$ 20 h	$Fe_{80}Cr_{20}$ 20 h	Milled 20 h and hot compacted
$Fe_{80}Cr_{20}$ 40 h	FC-1	Milled 40 h hot compacted and SPS processed
$Fe_{80}Cr_{20}$ 60 h	FC-2	Milled 60 h, hot compacted and SPS processed
$Fe_{80}Cr_{20}$ 80 h	FC-3	Milled 80 h, hot compacted and SPS processed
Commercial Ferritic steel	FC-4	Commercial Ferritic Steel
Fe powder	FC-5	Fe Powder
Cr powder	FC-6	Cr powder
$Fe_{80}Cr_{20}$ 40 h	FC-1La	FC-1 Implanted with La
$Fe_{80}Cr_{20}$ 60 h	FC-2La	FC-2 Implanted with La
Commercial Ferritic steel	FC-4La	FC-4 Implanted with La

RESULT AND DISCUSSION

Crystallite size and strain of ball milled powders can be seen following Table 2.

Table 2: Evaluation ball milled powders of $Fe_{80}Cr_{20}$

Unmilled and Milled powder	crystallite size (nm)	Strain (%)
$Fe_{80}Cr_{20}$ 15 h	57.77	0.0022
$Fe_{80}Cr_{20}$ 20 h	11.45	0.0041
FC-1	6.38	0.0009
FC-2	5.82	0.0017
FC-4	9.36	0.0022
FC-5	198	0.0038
FC-6	198	0.002

As shown in table 1 the unmilled and milled powders of $Fe_{80}Cr_{20}$ with the increasing milling time the size of the structure starts to decrease successively due to heavy plastic deformation [7]. Starts of plastic deformation crystallite size $Fe_{80}Cr_{20}$ in milling time of 80 h and smallest crystallite size in milling time of 60 h with 5.82 nm and strain of 0.0017%.

SEM on Consolidated Powders

Consolidation process an effective to removal porosity with the hot compaction processes that removing air from the powder body in order to obtain good interparticle bonding. The spark plasma sintering can to obtain a part having both high densities as well as to desire microstructure. SEM image for consolidated powders can be seen in Figure 1.

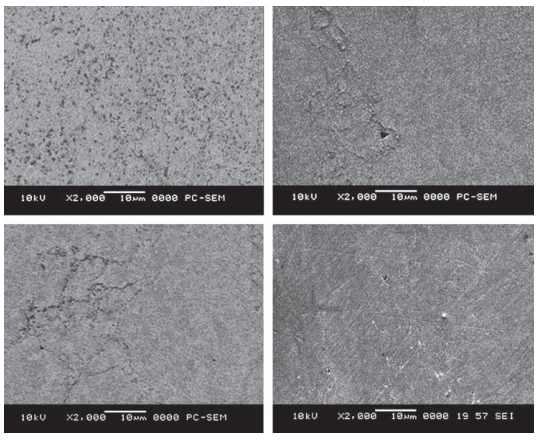

Figure 1 SEM images for the as consolidated (a) FC-1 (b) FC-2 (c) FC-3, and (d) FC-4

In this study, among the consolidation technique: SPS and HP, the SPS sample resulted in finer crystallite size than HP process which influenced by the reduction in an extensive grain

growth during sintering process. The results of the crystallite size calculation are also shown in Table 2. In HP sintering, it is more time consuming in order to achieve the sintered/consolidated alloy. The SPS samples were sintered with lower sintering temperature than HP process. However, the densification takes place much faster in the SPS than in HP process. The microstructure morphology of FC-1, FC-2, and FC-3 finer morphology structure than the FC-4, it can be seen from Figure-1 not identified the cracks and voids on consolidated specimens.

Oxidation resistance of La-implanted and unimplanted specimens

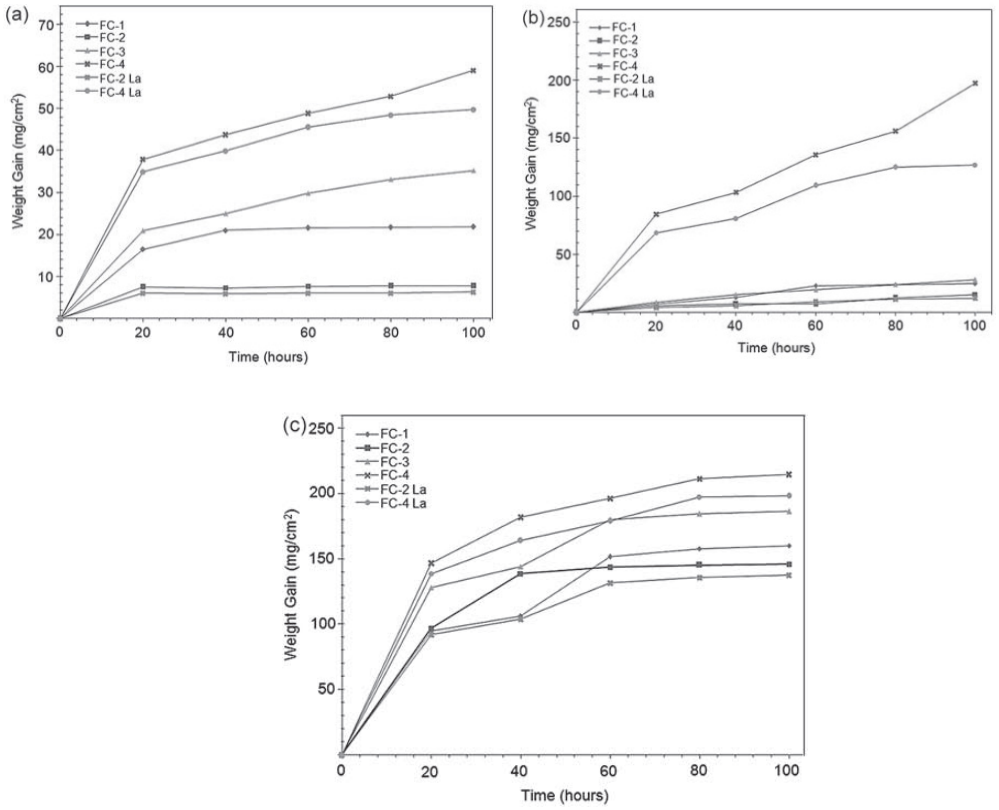

Figure 2: Mass gain as function of oxidation time for all the specimen La-implanted and unimplanted alloys oxidized at (a) 900 ^{0}C, (b) 1000 ^{0}C, (c) 1100 ^{0}C in air for 100 h

Figure 2 shown the mass gain for the sample oxidized at (a) 900 ^{0}C, (b) 1000 ^{0}C, (c) 1100 ^{0}C in air for 100 h of La-implanted and unimplanted. La-Implanted to all studied sample had an effect of reduction of oxidation. The mass gain for La-implanted alloy is reduced better than unimplanted alloy. The contribution of La implantation is also essential for the effectiveness of internal to external oxidation transition to form a continuous and slow growth oxide (chromium) layer. It also in oxidized at 1000 ^{0}C and 1100 ^{0}C in air for 100 h the effect of La-implanted better than unimplanted for reducing the mass gain of the $Fe_{80}Cr_{20}$ alloys. The parabolic oxidation model assumes that the oxidation process in diffusion limited. As none of the alloys, resulted in a parabolic rate constant within the required range, therefore further modifications are required in order for the alloys tested to be suitable for SOFC applications.

XRD pattern of La-implanted and unimplanted specimens

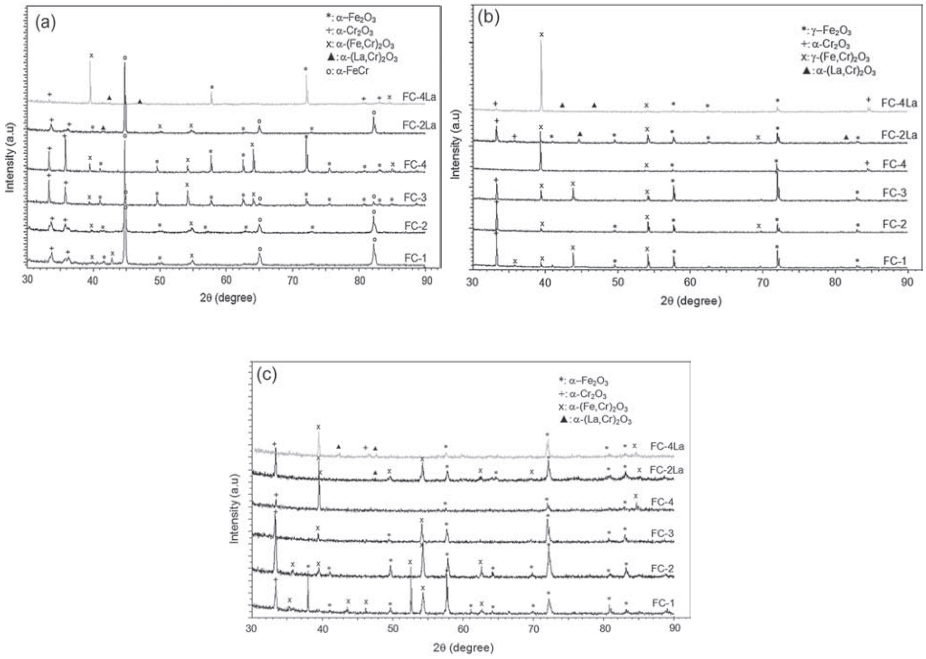

Figure 3: XRD patterns of La-implanted and unimplanted alloys at (a) 900 ^{0}C, (b) 1000 ^{0}C, (c) 1100 ^{0}C in air for 100 h

The XRD peaks also show the predominate phase in the oxide scales are Cr_2O_3 and $(Fe,Cr)_2O_3$ and also very weak peaks of Fe_2O_3. Meanwhile, the weak diffraction peaks observed the existence of La_2O_3 or $LaCrO_3$ only for the oxidized implanted samples. The XRD pattern for the unimplanted sample also indicated that mainly Cr_2O_3 is formed. Very week peaks of Fe_2O_3, $(Fe,Cr)_2O_3$ are also observed as this unimplanted samples Formation of Cr was very essential which offer potential as the protective oxide in order diminished the growth rate of oxide scale which usually spell under SOFC temperature operation condition [8]. The phenomenon may accrued due to the high oxygen pressure provides a driving forces for iron diffusion through the Cr scale as the interface oxide layer to form iron oxide. The early oxidation process with the oxide scale is very thin, the reaction speed is mainly controlled by the reaction speed at the interface until the final oxidation process is mainly controlled by diffusion because the increasing thickness of the scale by the path widens of oxygen diffusion. After the oxidation 1000 ^{0}C and 1100 ^{0}C the $Fe_{80}Cr_{20}$ alloys phase is no longer detected at all oxidized samples as the oxidation kinetics of the samples also increasing higher than the oxidation kinetics at 900 ^{0}C.

Microstructure morphology analysis with SEM and EDS result

Implanted specimens, the main oxide scale obtained were α-$(Fe, Cr)_2O_3$, α-Fe_2O_3, α-Cr_2O_3, and small amount of α-$(La, Cr)_2O_3$. The major phases of specimens after oxidation for 100 h at 1000 ^{0}C are illustrated at Fig. 5. For the unimplanted specimen, the main oxide scales obtained were -Fe_2O_3 and α-$(Fe, Cr)_2O_3$; and the minor oxide scale was α -Cr_2O_3. For the implanted specimens,

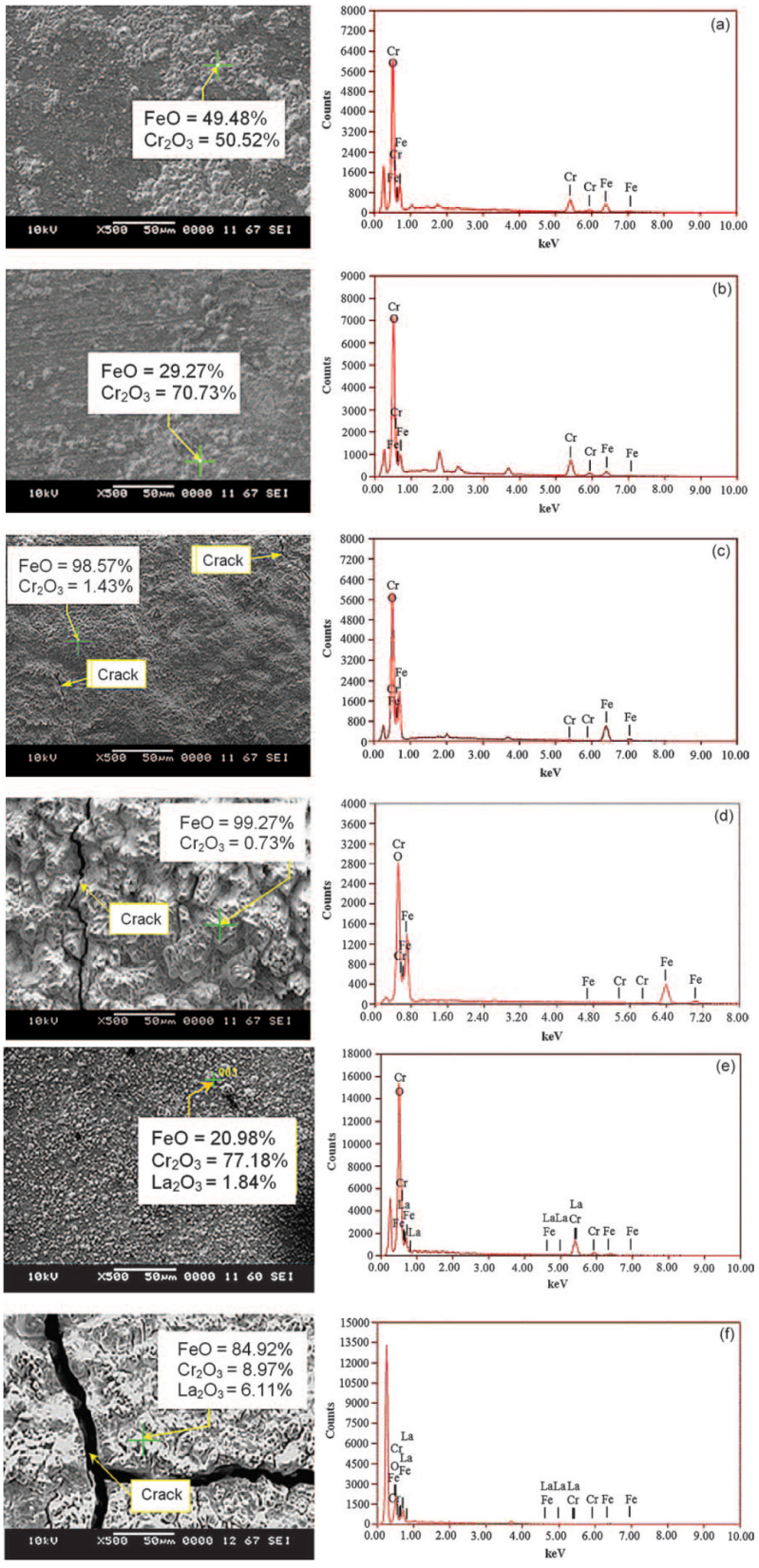

Figure 4: SEM oxide morphology and EDS results of the specimens after oxidation at 900 ^{0}C for 100 h: (a) FC-1, (b) FC-2, (c) FC-3, (d) FC-4, (e) FC-1La, and (f) FC-4La

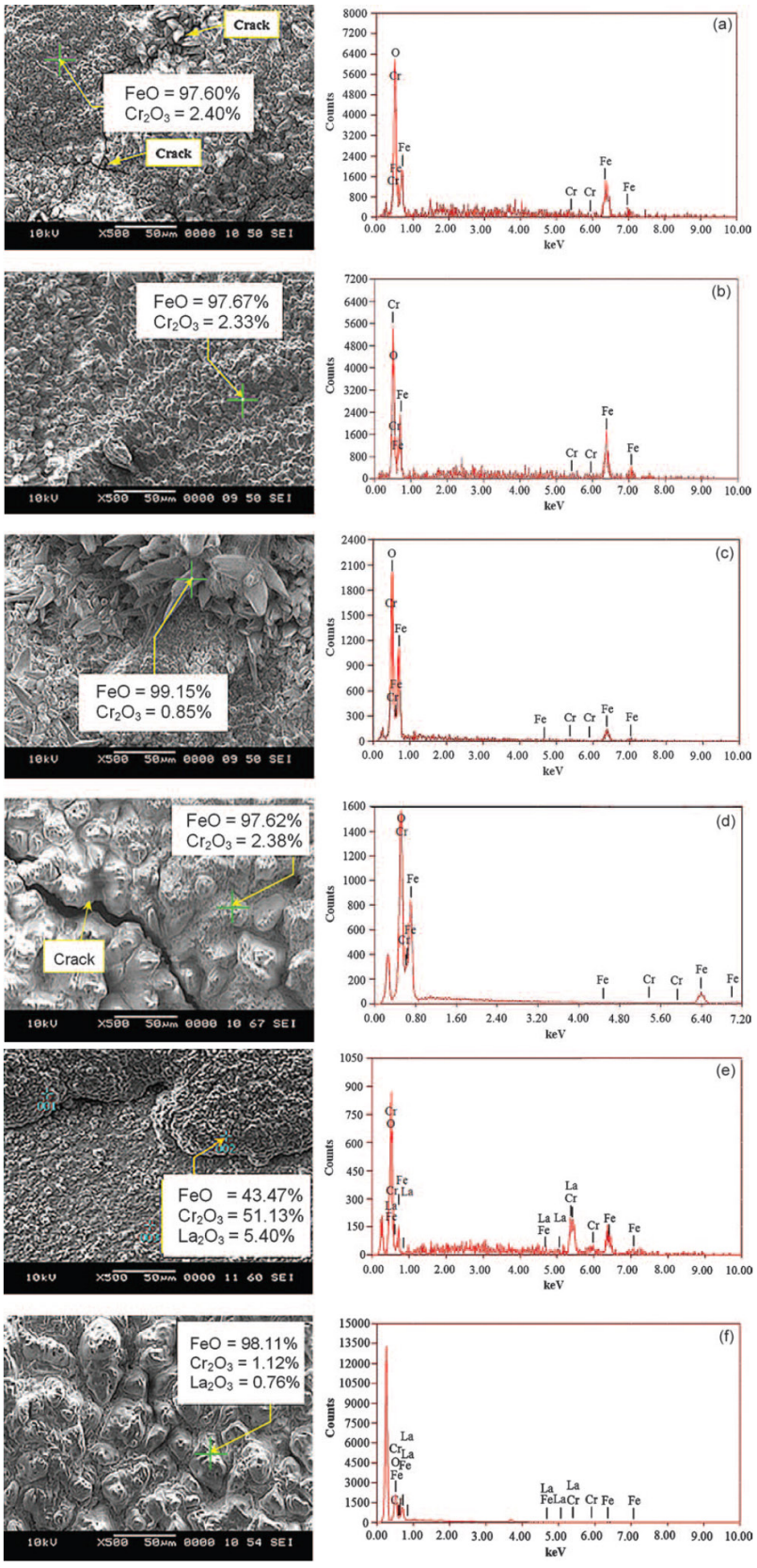

Figure 5: SEM oxide morphology and EDS results of the specimens after oxidation at 1000 ^{0}C for 100 h: (a) FC-1, (b) FC-2, (c) FC-3, (d) FC-4, (e) FC-1La, and (f) FC-4La

the main oxide scales obtained were -(Fe, Cr) $_2O_3$, α -Fe_2O_3, α-Cr_2O_3, and small amount of α-(La, Cr) $_2O_3$. After 100 h of exposure at 1100 ^{0}C, the main oxide scale consisted of α-Fe_2O_3, while α-(Fe, Cr)$_2O_3$ and α-Cr_2O_3 was obtained as the minor oxide scale for the unimplanted specimens. The major phases of the implanted specimens after oxidized for 100 h at 1100 ^{0}C were α-(Fe, Cr) $_2O_3$, α-Cr_2O_3, -Fe_2O_3, and minor phase of α-(La, Cr) $_2O_3$. The appearance of Fe_2O_3 as a thin layer at the scale/substrate interface reflects the higher thermodynamic stability of this oxide as compared to Cr_2O_3 for specimen FC-3 and FC-4 after oxidation at 1100 ^{0}C. For the as developed FeCr specimens, both unimplanted and implanted at 900 ^{0}C, it is evidenced that growing oxide peaks but still shows the peaks of the original specimens. It indicates that the oxidation growth at 900 ^{0}C on the surface of the as developed FeCr specimen that occurred but not significant [9].

SEM cross section

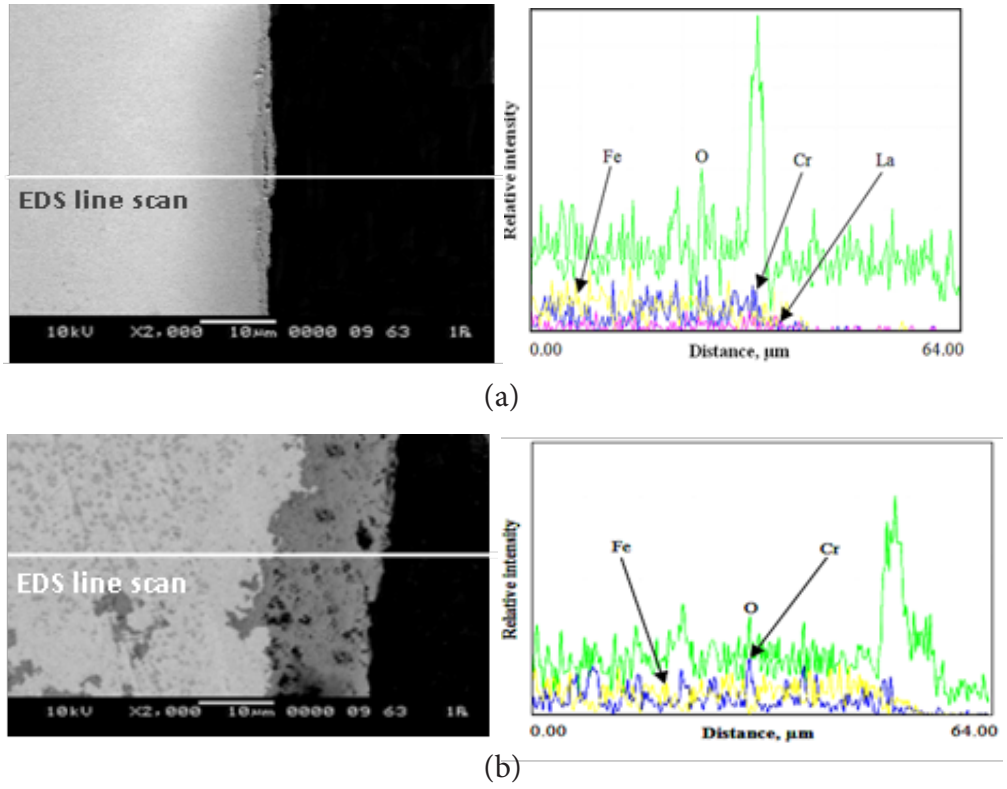

Figure 6: SEM Cross-section and EDS line scan profile of the implanted (a) SPS800 (b) Unimplanted HP1000 oxidized at 900 ^{0}C.

In the line scan show that O element peak present in the implanted SPS800 become decreased as indicated in figure 6-a. For the unimplanted sample, the thickness of FeCr HP1000 is approximately three times compared the thickness of SPS800 sample. As expected the lanthanum implanted samples exhibits a relative dense and continuous scale with relative strong adhesion to the substrate.

In the implanted and unimplanted samples, the cross section SEM after oxidation were better in the scale thickness, adherence, morphology, lower oxidation growth and clearly the oxide scale formed on substrate surface, the spallation crack and porous tend to accrued seriously. The

oxidation behaviour is sensitive to the microstructural characteristics of the materials, the improve oxidation resistance in the nanocrystalline because improved adhesion of passive film formed over nancrystalline structure. The ion implantation by La is primarily contribute to the adherence of oxide scale and the contribution of alloy surface treatment to the alloy is also essential for the effectiveness of internal to external oxidation transition to form a continuous oxide (Cr_2O_3) layer.

Electrical resistivity

Table 3: The electrical resistivity of the implanted and unimplanted specimens

Specimens	Electrical Resistivity (Ωcm)		
900 ^{0}C	1000 ^{0}C	1100 ^{0}C	1100 ^{0}C
Implanted			
SPS800	119.55	122.25	207.05
SPS900	119.7	124.7	208.18
HP1000	119.78	124.8	211.93
FC-4	145.8	146.05	224.18
Unimplanted			
SPS800	119.9	122.4	211.15
SPS900	120.15	124.93	217.55
HP1000	120.22	125.65	216.85
FC-4	146.65	146.2	225.57

According to the [10], the data for electrical properties of interconnect is typically evaluated by the area specific resistance (ASR). From the Table 3, it can be seen that the FC-4 materials have highest ASR values because the formations of oxide scale at the interface with the alloy. If compared the SPS800 and SPS900 samples show lower ASR values compared to the HP1000 sample. La implantation sample showed lower ASR values than unimplanted sample. That is caused of the reactive element effect, because the element improves the oxidation resistance of alloy and the formation of caution defects in the chromia scale, increasing subsequently the conductivity of the scale. In this study $Fe_{80}Cr_{20}$ alloys SPS800 after 100 h at below 1100 0C posses the lowest ASR values which is still much lower than the ASR limit values that the interconnect should posses and expected to be suitable as interconnect SOFC material.

CONCLUSION

The new process of this research is combining the multi process consist of ball milling process, hot compaction, spark plasma sintering and surface treatment via ion implantation. It indicated that this process produce good electrical resistance, good microstucture and good in high temperature oxidation for SOFC application.

ACKNOWLEDGMENTS

The authors thank to Ministry of Higher Education - Malaysia for financially supported by the FRGS Grant Scheme project.

REFERENCE

[1] Steele, B. C. H, Material Science and Engineering: The Anabling Technology for the Commercialization of Fuel Cell Systems. Journal of Materials Science, 36 (2001), pp. 1053-1068.

[2] Quadakkers, W.J., Abellan, J. P., Shemet, V., & Singheiser, L, Metallic Interconnector for Solid Oxide Fuel Cell-a Review. Materials at High Temperatures, 20(2) (2003), pp. 115-127.

[3] Khairudini, D. S, Development of Nanocrystalline Iron-Chromium Alloy by Means of Sintering and Ion Implantation for Interconnect Application in High Temperature Solid Oxide Fuel Cells. Faculty of Mechanical and Manufacturing Engineering, University Tun Hussein Onn Malaysia: Master Thesis, 2011.

[4] Omori, M, Sintering, Consolidation, Reaction and Crystal Growth by the Spark Plasma Sintering System (SPS). Material Science and Engineering A, 287 (2000), pp. 477-493.

[5] Cooper, L., Benhaddad, S., Wood, A., & Ivey, D. G, The Effect of Surface Treatment on the Oxidation of Ferritic Stainless Steel Used for Solid Oxide Fuel Cell Interconnects. Journal of Power Sources, 184 (2008), pp. 220-228.

[6] H. Saryanto, D. S Kairudini, P. Untoro & M. H. Saleh. Determination of nanocrystalline Fe80Cr20 based alloys using Williamson-hall Methode. Advanced materials research, 129-131 (2010), pp. 999-1003.

[7] Saryanto, H, High Temperature Resistance of Nanocrystalline Fe80Cr20 Alloys and Ferritic Steel Implanted with Lanthanum and Titanium, Faculty of Mechanical and Manufacturing Engineering, University Tun Hussein Onn Malaysia: Master Thesis, 2011.

[8] Sebayang, D., Deni S. Khaerudini, M.A. Othman, S. Hasan, S. Mahzan, D. Fredrick, T. Sujitno and P. Untoro, Comparison of High Temperature Oxidation of Nanocrystalline FeCr alloy Consolidated by Spark Plasma Sintering and Hot Pressing. World Journal of Engineering 2011, ISBN 1708-5284.

[9] Sebayang, D., Khaerudini, D. S., Saryanto, H., B. Omar, M. A. Othman., Hamid, A., Sujitno, T., and Untoro, P, Oxidation Resistance of Unimplanted and Implanted of Nanocrystalline FeCr Alloy and Commercial Alloy with Lanthanum. Journal of Advanced Microscopy Research Vol. 6 (2011), pp. 1–15.

[10] Zhu, W. Z. & Deevi, S. C, Opportunity of Metallic Interconnects for Solid Oxide Fuel Cells: a Status on Contact Resistance. Material Research Bulletin, 38 (2003), pp. 957-972.

Darwin Sebayang
Faculty of Engineering Technology, University Tun Hussein Onn Malaysia
Parit Raja, Batu Pahat, 86400 Johor, Malaysia
darwin@uthm.edu.my (+607-4537794)

Asraf Othman
Center for Diploma Studies, University Tun Hussein Onn Malaysia
Parit Raja, Batu Pahat, 86400 Johor, Malaysia
ashraf@uthm.edu.my (+607-4538605)

Maizlinda Izwana[a] & Dafit Feriyanto[b]
Faculty of Mechanical and Manufacturing Engineering
University Tun Hussein Onn Malaysia
Parit Raja, Batu Pahat, 86400 Johor, Malaysia
izwana@uthm.edu.my (+607-4538555)[a]
dafitferiyanto@yahoo.co.idd (011-230373-68)[b]

Deni S. Khaerudini4,e,
[4]Kawasan Puspiptek Serpong Tangerang, Indonesia 153000
seadick2000@yahoo.com (+81 80-4519-6601)

Hendi Saryanto5,f
[5]Jl. Perumahan Wisma Harapan Blok B.8 No.38, Priuk, Tanggerang, Banten, Indonesia.
mesin01@yahoo.com (+6281-76607576)